

Infrared photometry of the Local Group Dwarf Irregular Galaxy IC 10.

J. Borissova¹, L. Georgiev², M. Rosado², R. Kurtev³, A. Bullejos², and M. Valdez-Gutiérrez⁴

¹ Institute of Astronomy, Bulgarian Academy of Sciences, 72 Tsarigradsko chaussèe, BG – 1784 Sofia, Bulgaria
 email: jura@haemimont.bg

² Instituto de Astronomía, Universidad Nacional Autónoma de México, México
 email: georgiev@astroscu.unam.mx, margarit@astroscu.unam.mx

³ Department of Astronomy, Sofia University, BG – 1164 Sofia, Bulgaria
 email: kurtev@phys.uni-sofia.bg

⁴ Instituto Nacional de Astrofísica, Óptica y Electrónica, México
 mago@inaoep.mx

Received ; accepted

Key words: galaxies: individual: IC 10 – galaxies: Local Group – galaxies: stellar content – galaxies: kinematics

Abstract. We present the first deep near infrared *JHK* photometry for the central area of the irregular dwarf galaxy IC 10. The color-magnitude diagrams clearly show the presence of a red giant branch, an asymptotic giant branch and red supergiants. The metallicity $[Fe/H] = -1.60 \pm 0.27$ of the red giants in IC 10 is calculated using the slope of the giant branch. We also present the calculated foreground reddening $E(B - V) = 0.88 \pm 0.11$ and the distance modulus $(m - M)_0 = 24.0 \pm 0.2$ mag. Six Brγ emission structures have been detected thus tracing two star forming regions in the galaxy.

1. Introduction

IC 10 is an irregular dwarf member of the Local group. This galaxy is an extremely peculiar and interesting object. As pointed out by Hubble (1936): "The third nebula, IC 10 is one of the most curious objects in the sky. Mayall, at the Lick observatory, was the first to call attention to its peculiarities...The photographs are difficult to interpret fully, but they suggest that a portion of a large, late-type spiral is dimly seen between obscuring clouds".

Shostak et al. (1989) and Wilcots et al. (1998) have mapped the extended gas around the irregular galaxy IC 10. They have shown that the extended gas around this galaxy is also amazingly complex. Single-dish observations of IC 10 had suggested that the outer envelope was turbulent and there were velocity gradients at small and large scales (Cohen 1979), but the new VLA mosaic shows that the extended HI is concentrated in three arm-like structures and that IC 10 is merging with a large infalling cloud to the south of the disk (Hunter 1997).

Send offprint requests to: J. Borissova

The stellar content of IC 10 was investigated by several authors. Massey & Armandroff (1995) found a very well populated blue plume of main-sequence luminous stars in the $(V, B - V)$ color-magnitude diagram. They also found that IC 10 had a global surface density of Wolf-Rayet stars 3 times higher than any other Local Group galaxy. This high concentration of WR stars reinforces the idea that IC 10 is undergoing rather strong bursts of star formation. Saha et al. (1996) using Gunn g, r filters reported the existence of a blue plume containing the blue supergiants, a red vertical plume at $(g - r) = 1.3$ and other bright red supergiants redward of it. They also investigated the variable stars in IC 10 and reported four Cepheids. Wilson et al. (1996) confirmed the variability of these stars from IR photometry. Sakai et al. (1998) identified a well populated red giant branch, an ill-defined blue main sequence population and an intermediate-age asymptotic giant branch. Each of the above works reported different values of the distance modulus and the reddening, varying from $E(B - V) = 0.75$ to 1.16 and $(m - M) = 23.5$ to 24.9 . The calculations of reddening and distance reported above are based on different stellar population types – Wolf-Rayet stars (Massey & Armandroff 1995), Cepheid variables (Saha et al. 1996; Wilson et al. 1996) and the tip of the red giant branch method (Sakai et al. 1998). The most probable explanation of these so different results is that IC 10 lies extremely close to the Galactic plane thus having a high optical foreground reddening. Another possible reason for these differences could be the fact that since this is a starburst galaxy it has a variable internal reddening.

This paper presents the first *JHK* photometry of the central area of IC 10. The purposes of our work are to determine the stellar content, the reddening, the distance modulus and the ages of different stellar populations in IC 10 by means of an approach which is less sensitive to

both the foreground and the internal reddening and is at the same time sensitive to the star - formation activity - near IR observations.

Our observational material and data reduction techniques are described in Section 2 together with our analysis of the photometric errors and completeness corrections. Several aspects of the color - magnitude diagrams (CMD) of IC 10 including analysis of stellar content are described in Section 4. The metallicity of IC 10 as determined from photometric indicators is discussed in Section 5. IC 10's reddening, distance modulus and age are determined in Section 6 and Section 7. The recent star formation activity based on the $\text{Br}\gamma$ emission is analyzed in Section 8 and in Section 9 we summarize the most important results of the present investigation.

2. Observations and data reduction

2.1. JHK and UBV observations

The data discussed here were acquired with the Infrared Camera "CAMILA" (Cruz-González et al. 1996) with a NICMOS3 (256×256 pixels) detector attached to the 2.1-m telescope of the Observatorio Astronómico Nacional "San Pedro Martir", México. The scale was 0.85 arcsec/pixel, resulting in a field size of about 3.6 by 3.6 arcmin. A set of JHK frames was taken on January 11-13, 1998. JHK images of the Local group irregular galaxy IC 1613 were being taken throughout the same nights for comparison purposes. An additional set of short exposure (30 sec) UBV frames of IC 10 were obtained on the 2-m Ritchey-Chretien telescope of the Bulgarian National Astronomical Observatory on July 24, 1998 with a Photometrics 1024×1024 camera.

Twelve UKIRT (Casali & Hawarden 1992) standard stars as well as Landolt (1992) standards were taken before and after all observations.

The IRAF data reduction package was used to carry out the basic image reduction. The stellar photometry of the frames was done using DAOPHOT II (Stetson 1993).

In order to estimate the internal accuracy of our photometry we used the formal errors from the DAOPHOT package. For all stars the standard errors vs. magnitudes are displayed in Fig. 1. As can be seen we do not have large errors (> 0.25) up to the fainter magnitudes: $J > 18.0$, $H > 17.5$ and $K > 18.5$.

The artificial star technique (Stetson 1991) was used to outline the limits of our photometry and series of artificial frames were reduced in the same manner as the original frames. We estimate our completeness limits to be 17.0 magnitudes in J and 16.5 magnitudes in H and K .

2.2. $\text{Br}\gamma$ and H_2 observations

Narrow band imaging in the $2.17\mu\text{m}$ $\text{Br}\gamma$, $2.12\mu\text{m}$ $v = 1 - 0$ $\text{S}(1)$ H_2 and $2.26\mu\text{m}$ continuum lines was carried

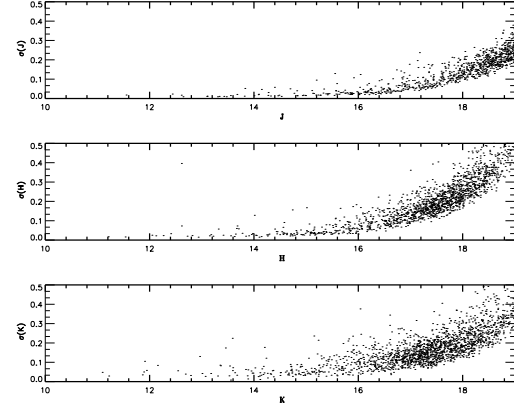


Fig. 1. Internal errors of the IC 10 photometry.

out on the last night of the same observational run in "San Pedro Martir" observatory — 13 January 1998. The atmospheric conditions were stable. Flux calibration was made using the WD atmosphere model of the faint ESO DA0 spectrophotometric standard star G191-B2B (Oke 1990, Bohlin et al. 1995). Images of the standard star were taken at the same airmasses as the program fields.

3. Comparison with previous works

Unfortunately there are only two papers on the IR-photometry of IC 10 and IC 1613 and they deal with a few stars only — Wilson et al. (1996) and Elias & Flogel (1985).

There is only one star from our field of observations that is present in the infrared IC 10 data of Wilson et al. (1996) — the very red variable star V3. The difference in $J - K$ color is $(J - K)_{\text{our}} - (J - K)_{\text{Wilson}} = 0.01$ and in K magnitude is $K_{\text{our}} - K_{\text{Wilson}} = 0.06$.

There are two stars common for our and Elias & Flogel's (1985) IR photometry of IC 1613 — the well known variable red supergiants V32 and V38 (Sandage 1971). Elias & Flogel (1985) give observed colors and magnitudes for V32 and V38 $J - K = 0.87$, $K = 13.12$ and $J - K = 0.84$, $K = 13.12$, respectively. The differences between our data and that of Elias & Flogel are 0.1 in K and 0.05 in $J - K$ for both stars.

Taking into account that V3 in IC 10 and V32 and V38 in IC 1613 are variable stars we have a very good agreement between our data and that of Wilson et al. (1996) and Elias & Flogel (1985).

4. Color-magnitude diagrams

Fig. 2, Fig. 3 and Fig. 4 show the $(J - K, K)$, $(H - K, K)$ and $(H - K, J - H)$ color-magnitude and color-color diagrams obtained for IC 10. Only stars with photometric

errors less than 0.25 were selected in all filters. Our final list contains 1036 sources with J , H and K magnitudes.

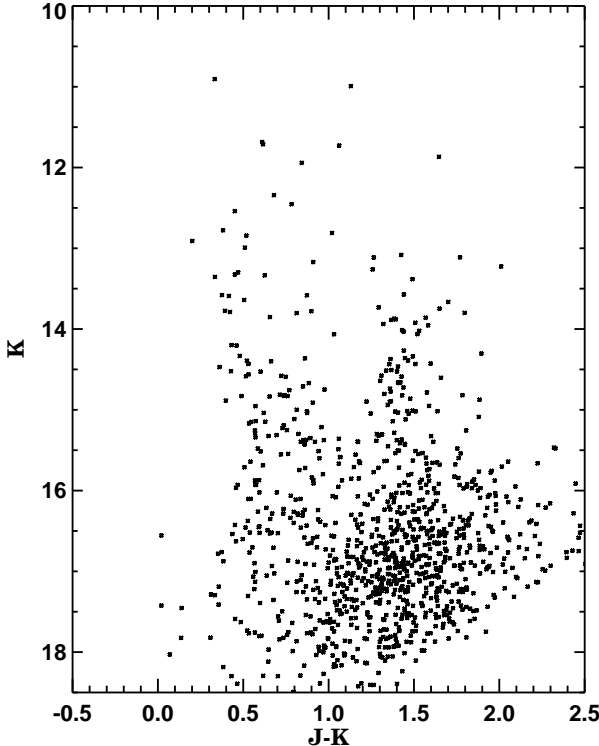


Fig. 2. ($J - K, K$) color-magnitude diagram obtained for IC 10.

It is well known that the main features of the red color-magnitude diagrams are the red giant branch (RGB), the asymptotic giant branch (AGB) and the red supergiants (RSG).

It is obviously necessary however to check the level of field star contamination before discussing the detailed structure of the color-magnitude diagrams and the stellar content of the IC 10.

4.1. Field star contamination

IC 10 is practically situated in the galactic plane ($b = -3^{\circ}34$, $l = 118^{\circ}97$) and the foreground contamination is significant. To locate the field stars on the color-magnitude diagrams we used three different methods : the Bahcall & Soneira (1980) model, specially designed for field star analysis at very short exposure times (30 sec), UBV CCD frames and a JHK comparison file.

Fig. 5 shows the ($B - V, V$) color-magnitude diagram. Taking into account the distance modulus of IC 10 we can expect that 90% of the stars from our short exposure time CCD frames are field stars. Using the Bahcall & Soneira (1980) model of the Galaxy we calculated the number of expected field objects per bin of magnitude and color in

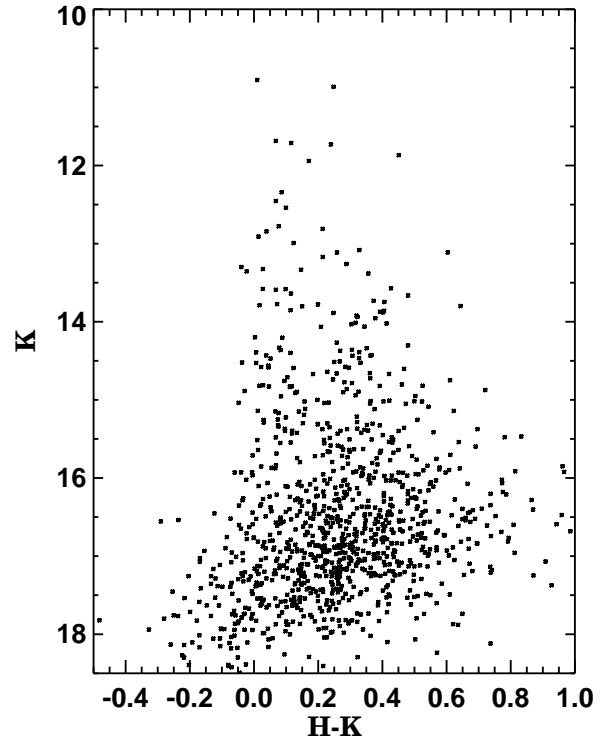


Fig. 3. ($H - K, K$) color-magnitude diagram obtained for IC 10.

the area covered by our observations. The predicted number of field stars is superimposed on Fig. 5. As can be easily seen most of the stars with $V < 21$ and $B - V > 0.8$ are really field stars. The few most luminous stars from the blue plume are located close to $B - V = 0.6$, $21 > V > 19$ and the few most luminous stars from the red plume are located around $B - V = 1.3$, $21 > V > 19$.

These results agree with the analysis of Massey & Armandroff (1995) who found the blue plume at $B - V = 0.6$ and field stars around $B - V = 1.0$ and $V = 17$ mag.

We then statistically decontaminated the observed CMD by applying the following procedure: the CMD was subdivided into 15 boxes (shown in Fig. 5) — five intervals in magnitude and three in color. The "candidate" field stars were randomly subtracted from the CMD sample in each box up to the predicted from Bahcall & Soneira (1980) model number. The subtracted field stars were cross-identified with the IR photometry data and were superimposed on the $J - K, K$ color-magnitude diagram in Fig. 6 as squares.

As a second attempt to localize the field stars we used the JHK images. Our images cover 3.6×3.6 arcmin (256×256 pixels). The galaxy is oriented NW-SE and the north-east corner of the field of observations is almost free of galaxy stars. There are only foreground stars and a few stars from IC 10's halo in this area (Sakai et al. 1998). We

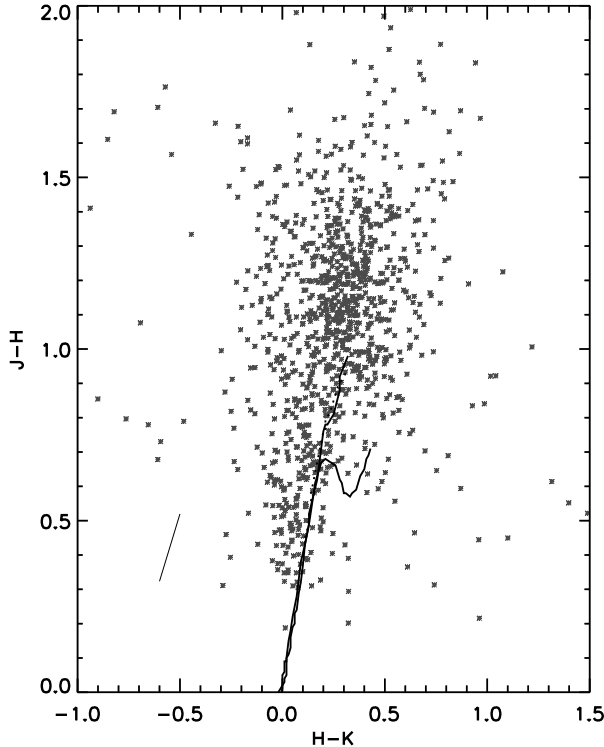


Fig. 4. $(H - K, J - H)$ color-color diagram obtained for IC 10. The mean lines for main sequence and supergiants from Koornneef (1983) were superimposed. The reddening vector for $A_V = 1$ is also shown.

used this region as a comparison field (64×64 pixels). On Fig. 6 we overplot the stars in that corner as circles.

The analysis of Fig. 6 shows that most of the stars between $0.6 < J - K < 1.0$ and $0.1 < H - K$ are field stars while stars with $J - K$ colors greater than 1 and $H - K > 0.1$ belong to IC 10 and only few field stars fall in the latter zone.

4.2. Theoretical H-R diagram

One of the best ways to analyze the stellar content of a galaxy is to put its stars on the theoretical H-R diagram. The comparison with theoretical evolutionary mass tracks predicted by theoretical models will give us the evolutionary stage of each star.

To plot the stars on the theoretical H-R diagram we need to determine their effective temperatures (T_{eff}) and bolometric corrections (BC). As we already pointed out in the Introduction there are numerous values for reddening and distance modulus for IC 10 varying from 830 kpc to 3 Mpc and $E(V - B)$ varying from 0.64 to 2.0 (for more details see Sakai et al. (1998) and the references therein).

Since our analysis is based on IR data we chose as a starting point the values obtained by Sakai et al. (1998)

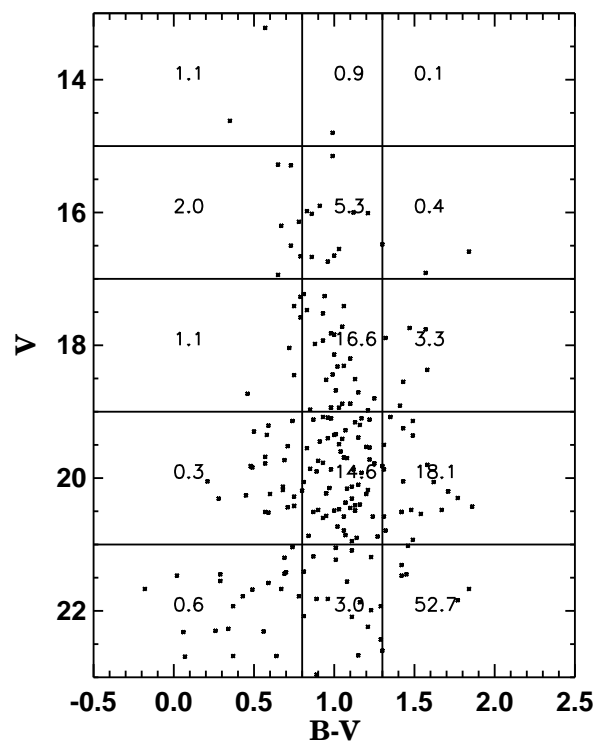


Fig. 5. $(B - V, V)$ color-magnitude diagram for IC 10. The predicted field stars per bin of magnitude and color from Bahcall & Soneira (1980) model are given.

based on red giant stars: $E(B - V) = 0.85$ and $(m - M) = 24.1 \pm 0.2$.

The only value for the metallicity of IC 10 that we could find was determined from the observation of HII regions and is reported to be $12 + \log(\text{O/H}) = 8.2$, which is close to the metallicities of NGC 6822 and IC 1613.

We used Costa & Frogel's (1996) method to transform K magnitudes and $(J - K)$ colors into M_{bol} and (T_{eff}) .

We first transformed our K magnitudes and $J - K$ colors into the CIT system by means of equations 1 and 2 derived by Ruelas-Mayorga (1997) for the Mexican set of filters. Then using equation 6 from Costa & Frogel (1996) we transformed our $(J - K)_{\text{CIT}}$ colors to the Johnson system. The bolometric correction for the K magnitude was calculated using their equation 1, while T_{eff} for each star was derived as the mean value of the temperatures given by their equations 8 and 9. The resulting H-R diagram is shown in Fig. 7. The evolutionary mass tracks from Charbonnel et al. (1993) for $z = 0.004$ were superimposed on the same plot.

To test our transformations we built the H-R diagram for a selected area of IC 1613 centered on the HII regions of the northeast sector of the galaxy using the same method. IC 1613 has a very low reddening $E(B - V) = 0.03 - 0.06$ (Sandage 1971; Freedman 1988; Georgiev et al. 1999),

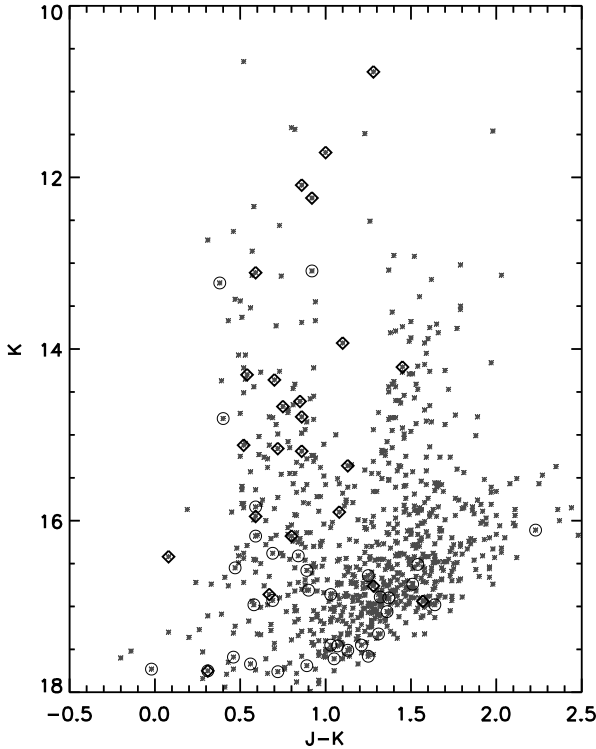


Fig. 6. $(J - K, K)$ color-magnitude diagram for IC 10. The predicted field stars per bin of magnitude and color from Bahcall & Soneira (1980) model are shown as open squares and the field stars from the comparison field (see text) are plotted as open circles.

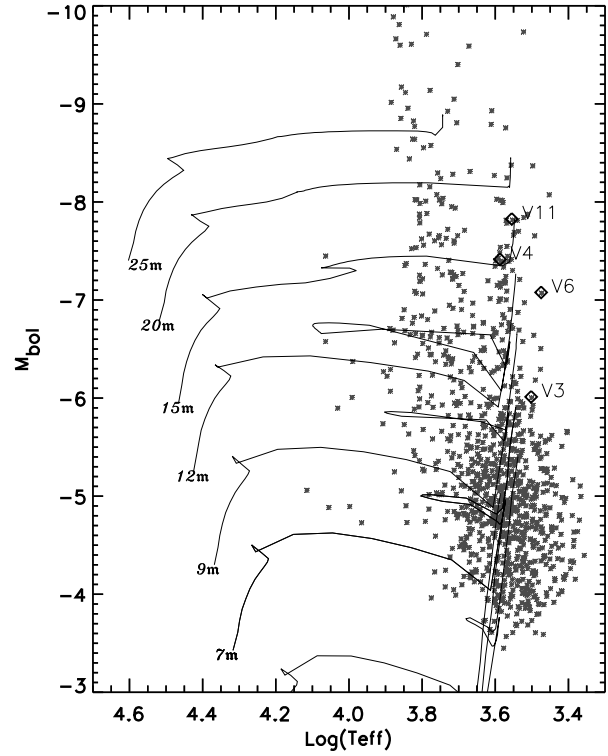


Fig. 7. H-R diagram for all stars in IC 10. The evolutionary mass tracks from Charbonnel et al. (1993) for $z = 0.004$ are superimposed on the same plot. Four variable stars are marked by open squares.

the field contamination from our Galaxy is negligible (Georgiev et al. 1999) and it has a relatively well known distance — $(m - M) = 24.2 \pm 0.2$ (Freedman 1988, Saha et al. 1992). The H-R diagram for IC 1613 is shown in Fig. 8. As can be seen the red giant stars lie between 5 to 7 M_{\odot} and the two very bright stars with 20 M_{\odot} are the red irregular variables V32 and V38 (Sandage 1971). The derived effective temperatures of V32 and V38 are approx. 3900 K, which is in agreement with their M0Ia spectral class (Elias & Flogel 1985).

Returning to the H-R diagram of IC 10 (Fig. 7) we can see the giant branch stars which match very well the evolutionary track with masses from 5 to 7 M_{\odot} . Using the above adopted reddening and distance the tip of RGB can be located at $M_{\text{bol}} = -4.7$.

The other main feature of the red diagrams is the asymptotic giant branch (AGB). It is not possible to separate the AGB stars from the RSG ones by means of JHK photometry only. Sakai et al. (1998) found the AGB stars in IC 10 to be "slightly brighter than the RGB stars". On our H-R diagram these stars can be located up to $M_{\text{bol}} = -6.5$

The stars between 12 and 25 M_{\odot} can be identified as red supergiants. With no spectra available we calculated the effective temperatures and M_{bol} for all variable stars in our field in order to check whether the red supergiants were correctly located on the H-R diagram. Saha et al. (1996) and Wilson et al. (1996) determined the light curves and periods for 13 variable stars. Four of them were found to be Cepheides. Unfortunately only four of these variables are measured in our photometry — V3, V4, V6 and V11. There are no Cepheid variables among them. V4 and V6 were found by Saha et al. (1996) to be eclipsing variables. V3 is a very red variable star with $P = 7.1123$ whose status is unclear. V11 stands in the $(r - i, r)$ diagram of Saha et al. (1996) (see their Figure 7) among the red supergiants and has been classified by Saha et al. (1996) as a Cepheid-like variable with a very long period ($P = 90.70$ days). On Fig. 7 these stars are marked by open squares. As can be seen V11 has $M_{\text{bol}} = -7.5$, $\text{Log}(T_{\text{eff}}) = 3.7$ and $15 M_{\odot}$. We consider the stars between $-6.5 < M_{\text{bol}} < -9$, $3.5 < \text{Log}(T_{\text{eff}}) < 3.7$ with masses greater than $12 M_{\odot}$ to be red supergiants.

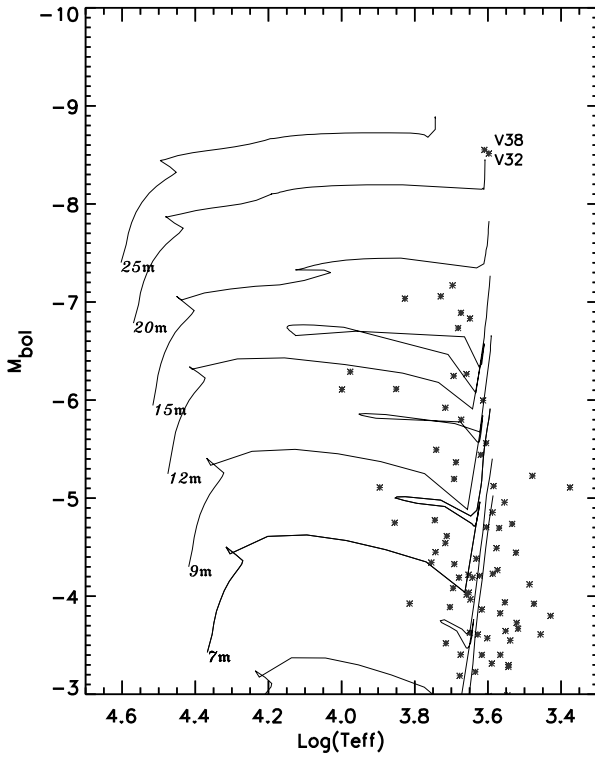


Fig. 8. H-R diagram for IC 1613. The evolutionary mass tracks from Charbonnel et al. (1993) for $z = 0.004$ are superimposed on the same plot. Red variable stars V32 and V38 are labeled.

5. Metallicity

We can derive a photometric estimate of the metallicity of a galaxy from the overall morphology of the infrared GB. It is well known (see for example Braun et al. 1998) that $(J - K)_0$ and $(V - K)_0$ colors are sensitive to metallicity, while $(H - K)_0$ is solely a function of the temperature (T_{eff}). Kuchinski et al. (1995) and Kuchinski & Frogel (1995) demonstrated both empirically and theoretically that the slope of the upper giant branch in the K vs. $(J - K)$ diagram is sensitive to the metallicity of the population for the metal-rich galactic globular clusters. Tiede et al. (1997) extend this relation to a sample of open clusters and bulge stars. They also found that a slope of giant branch is reddening - free parameter and using relatively large sample of galactic globular clusters calculated the relationship between $[Fe/H]$ and giant branch (GB) slope.

We used their calibration equation: $[Fe/H] = -2.98 - 23.84(\text{GBslope})$ to calculate the metallicity of the IC 10 giants.

We first had to separate the giants belonging to the upper giant branch. According to Tiede et al. (1997) for our Galaxy these are exactly the stars that have absolute K magnitudes in the range of $-2 < M_K < -6.5$ and $3.5 < \text{Log}(T_{\text{eff}}) < 3.7$.

We can not use directly these criteria because our photometry is not deep enough but we can use the basic idea — to select the stars belonging to the upper giant branch. On the theoretical H-R diagram we selected all stars with $3.5 < \text{Log}(T_{\text{eff}}) < 3.7$ and $-6.0 < M_{\text{bol}} < -4.0$ in the mass interval between 5 and $7 M_{\odot}$ (see Fig. 8). We chose this relatively wide range in M_{bol} putting in our calculation a 0.5 mag uncertainty for $(m - M)$. The least-squares fit to the above selected giants in the observational (not corrected for reddening and distance modulus) $(J - K, K)$ color-magnitude diagram was then performed and the best fit was $(J - K) = 2.42 - 0.058 K$.

The formal std error of the fit was estimated to be ± 0.11 . The giant branch slope value of -0.058 gives $[Fe/H] = -1.60 \pm 0.27$. The error of $[Fe/H]$ was derived from a combination of the error given by Kuchinski & Frogel (1995) and the formal least-squares fit error.

We used again the well studied IC 1613 to verify our method. The result was $(J - K) = 1.36 - 0.05 K$ with formal std error $\sigma = 0.04$ and a resultant metallicity $[Fe/H] = -1.79 \pm 0.25$. This value is in good agreement with the metallicity value measured for IC 1613 by Kingsburgh & Barlow (1995).

We can therefore assume that the red giants in IC 10 and IC 1613 have similar metallicities within the estimated error range.

6. Revised Reddening and Distance

We can now redetermine the reddening and the distance modulus of IC 10 comparing the red giants and the red supergiants in IC 10 and IC 1613.

The above mean line for the upper giant branch of IC 1613 was corrected for reddening and matched with the corresponding mean line for IC 10 by minimizing the std error.

The resultant differences are : $(J - K)_{\text{IC}1613} - (J - K)_{\text{IC}10} = -0.49 \pm 0.11$ and $K_{\text{IC}1613} - K_{\text{IC}10} = 0.74 \pm 0.3$. Since the two galaxies have similar giant branch metallicities and the red giants for both galaxies are chosen to have the same mass interval we believe that these differences are due to their different reddening and distance only. Using the relation $E(J - K) = 0.56 E(B - V)$ (Bessell & Brett, 1988) and the IC 1613 distance modulus value $(m - M) = 24.2$ we could calculate the reddening and the distance modulus of IC 10: $E(B - V) = 0.88 \pm 0.11$ and $(m - M)_0 = 23.8 \pm 0.3$.

The superimposition of the dereddened color-magnitude diagrams of the two galaxies is shown in Fig. 9.

Elias et al. (1981) demonstrated that infrared photometry of M supergiants does not provide by itself reliable distances to galaxies because the stellar K magnitude depends on galaxian luminosity and metallicity. In our case we have two galaxies with similar luminosity and metallicity. According to Mateo (1998) IC 10 has a total magnitude $M_V = -15.7$ and IC 1613 has $M_V = -14.7$. Most

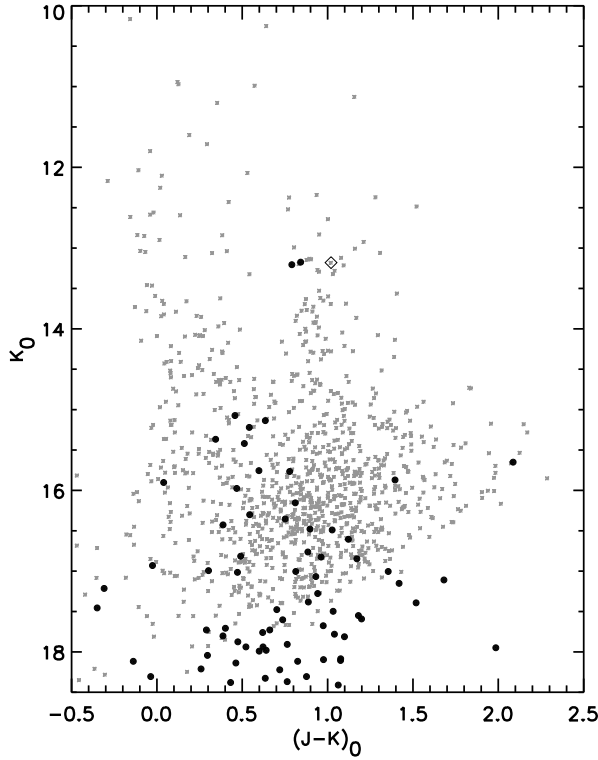


Fig. 9. Superimposed color - magnitude diagrams of IC 10 (light circles) and IC 1613 (dark circles). The red variable star V11 is shown by an open square. IC 1613 is corrected for reddening. IC 10 is shifted with $\delta(J - K) = -0.49$ and $\delta K = 0.74$.

of the red supergiants are known variables at visual wavelengths but there are no large variations in the infrared — typically 0.1 mag and less in K . We can now compare the red supergiants of the two galaxies. Irrespective of the very similar metallicities derived for both galaxies the $(K, H - K)$ color magnitude diagrams were used to minimize the metallicity effects. The mean $H - K$ and K values for the two red variables V38 and V32 of IC 1613 were corrected for reddening ($E(B - V) = 0.06$) and compared with the mean values of seven red supergiants in IC 10 standing around $H - K = 0.35$ and $K = 14$. Based on the assumption that reddening is the only reason for the differences between the colors of the red supergiants of the two galaxies we derived $E(H - K) = 0.24 \pm 0.09$ mag. This value corresponds to $E(B - V) = 1.26 \pm 0.19$ mag, using the relation $E(H - K)/E(B - V) = 0.19$ (Bessell & Brett 1988). We can now calculate the distance modulus $(m - M)_0 = 23.9 \pm 0.13$ for IC 10 from the corresponding differences in the dereddened K magnitudes.

The superimposition of the dereddened color-magnitude diagrams of the two galaxies is shown in Fig. 10.

An alternative method to determine the mean reddening is to use several blue stars from main sequence in the

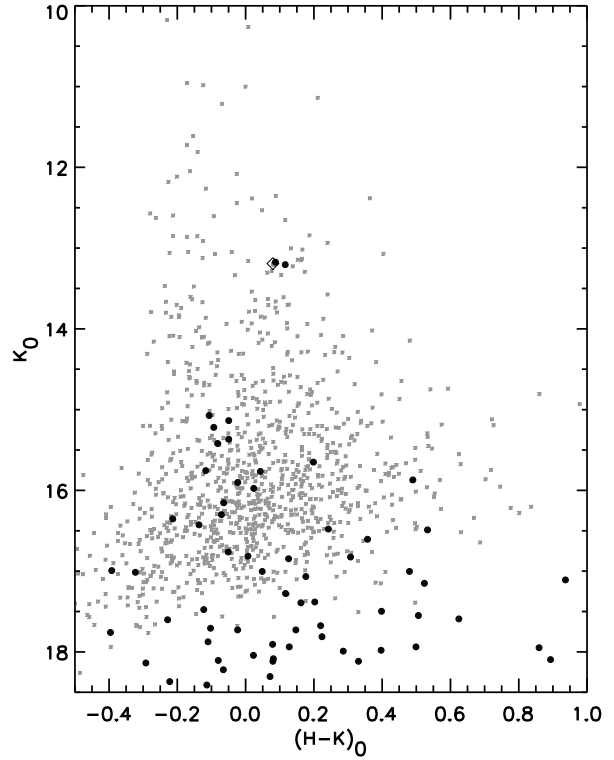


Fig. 10. Superimposed color - magnitude diagrams of IC 10 (light circles) and IC 1613 (dark circles). The red variable star V11 is shown by an open square. IC 1613 is corrected for reddening. IC 10 is shifted with $\delta(H - K) = 0.24$ and $\delta K = 0.3$.

UBV photometry. We used Johnson's Q -parameter technique to measure the reddening ($Q = (U - B) - 0.72(B - V)$ is a reddening-free quantity), calculating the Q values for all stars belonging to the main sequence (luminosity class V). These stars stand at V -magnitudes between 19 and 21 mag and in $U - B$ colors between -1.2 and 0. The $E(B - V)$ for each star was calculated using the equations given in Massey et al. (1995). We will assume that the "mean" value for $E(B - V)$ in this area of IC 10 is the average of the above determined individual $E(B - V)$ values. Our final value for $E(B - V)$ is 0.78 with $\sigma = 0.15$.

The histogram on Fig. 11 shows both the differential and the cumulative luminosity function for all stars (corrected for completeness) with $J - K$ colors greater than 1.0. Two peaks can be located on the histograms — at $K = 16.1 \pm 0.1$ and at $K = 16.9 \pm 0.1$. We believe that the first peak represents the AGB population in IC 10 and the second one marks the tip of the red giant branch. Following the method of Sakai et al. (1998) we calculated the distance modulus using the calibration equation $(m - M)_K = K_{\text{TRGB}} - M_{\text{bol}} + BC$. As a result we obtained $(m - M)_K = 24.1 \pm 0.3$ from the assumed reddening $E(B - V) = 0.88$ and $[\text{Fe}/\text{H}] = -1.60$. The er-

ror was calculated as a combination of the tip position, the reddening and the TRGB calibration errors.

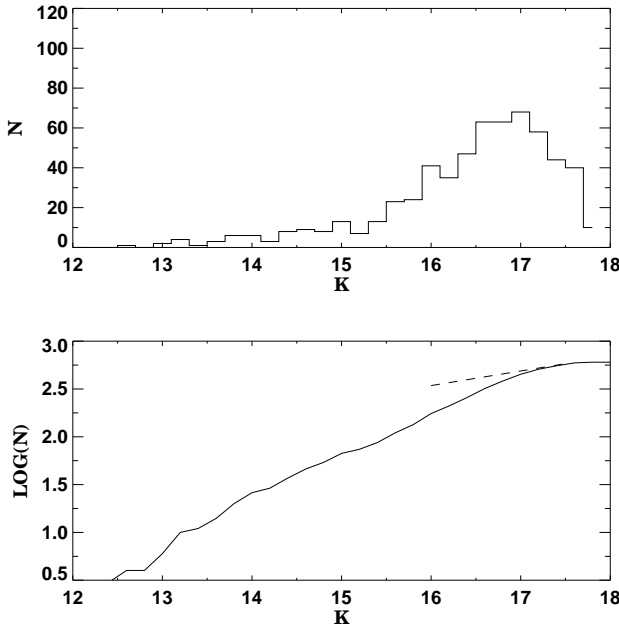


Fig. 11. The differential and the cumulative luminosity function for all stars with $J - K$ colors grater than 1.0.

The reddening values obtained by the three different methods — the comparison of the upper parts of the giant branches, the comparison of the red supergiants and the UBV photometry of the blue main sequence stars are substantially different. The UBV photometry of the blue main sequence stars yields the lowest reddening value $E(B - V) = 0.78 \pm 15$. This is easily explained by the fact that our very short exposure frames register only the brightest blue stars from the front of the galaxy. The position of the red supergiants in IC 10 indicates that they are located in deeply embedded in gas areas and have therefore the greatest reddening. Finally the red giants are almost uniformly distributed throughout the galaxy thus yielding an intermediate reddening value. These three results actually confirm the variable internal reddening of IC 10.

We assume that the mean foreground reddening of IC 10 is $E(B - V) = 0.88 \pm 0.11$ and that the dereddened distance modulus is 24.0 ± 0.2 mag. These values are very close to the values reported by Sakai et al. (1998).

7. Age

The next step in our analysis was to determine the age interval of IC 10. We used the $(K, H - K)$ color magnitude diagram to minimize the metallicity effects assuming $z = 0.004$, $E(B - V) = 0.88$ and $(m - M) = 24.0$ and

superimposing the isochrones for 10^7 , 10^8 , 10^9 and 10^{10} years from Padua's library (see Bertelli et al. 1994).

The analysis of the superimposed isochrones (Fig. 12) indicates that the red supergiants have ages between 50 and 100 Myr. The unambiguous presence of young red supergiant population corresponds to the presence of a large number of WR stars and the hypothesis of recent star burst formation. The red giants have ages of about 1 Gyr. Some older red giants can be seen with ages of several Gyr. Their real presence however can only be confirmed by a deeper photometry.

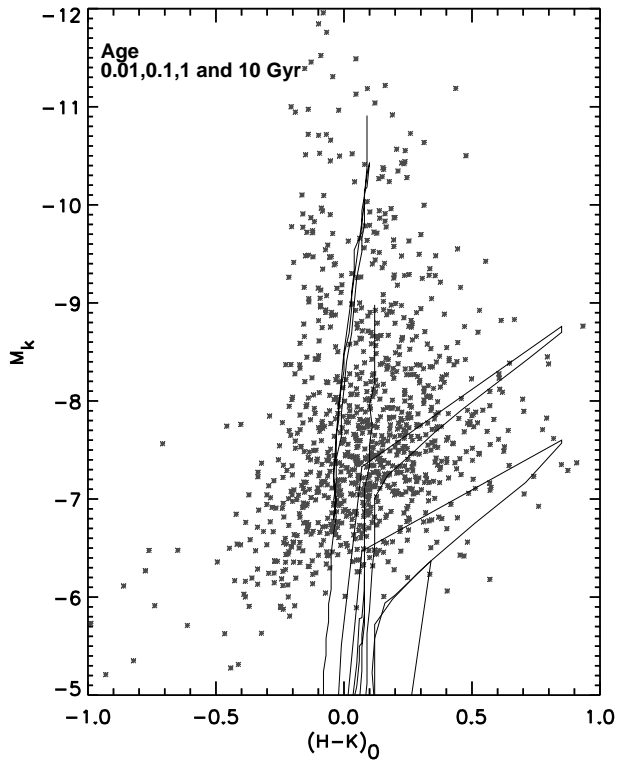


Fig. 12. The $(M_K, (H - K)_0)$ color-magnitude diagram of IC 10 with superimposed isochrones from Padua's library.

We can now return to the analysis of the stellar population in IC 10. Looking at the color-magnitude and color-color diagrams (Fig. 2, Fig. 3 and Fig. 4), the red giants and the AGB stars are visible at $J - K > 1.1$, $0.2 < H - K < 0.4$, $K > 14$ and the red supergiants stand around $J - K = 1.5$ and $13 < K < 14$ mag. Around $0.6 < J - K < 1.0$ and $0.1 < H - K < 0.2$ are located the field stars from our Galaxy. The second much older population of red giant stars may be present at $J - K = 1.8 - 2.0$. Our photometry is not deep enough to see any main sequence stars there.

8. Survey of star forming regions in IC 10

The near infrared *JHK* images can be used as continuum images which represent stellar light and hot dust emission from HII region complexes and dust extinction.

A red-green-blue composite true color image generated from our J (blue), H (green) and K (red) images is shown in Fig. 13. Several structures with infrared excess appear in the composite image, located in two regions named Zone 1 and Zone 2. The reddest object in Zone 1 is rather compact and has a mean diameter of 6 arcsec. Zone 1 also contains two fainter, extended and diffuse structures. Several stellar-like objects embedded into diffuse structures can be identified in Zone 2.



Fig. 13. The red-green-blue composite true color image generated from the J (blue), H (green) and K (red) images. North is at the top and east to the left. The field of view as shown is 3.6 arcmin.

A red-green-blue composite true color image generated from the $2.122\mu\text{m}$ H_2 (blue), $2.26\mu\text{m}$ continuum (green) and $2.165\mu\text{m}$ $\text{Br}\gamma$ (red) images is shown in Fig. 14. The emission structures in $\text{Br}\gamma$ are clearly visible (almost pure red) on this composite image and they coincide with the clearly visible (red again) infrared excess structures on the true color *KHK* image (Fig. 13).

A $\text{Br}\gamma$ image with subtracted continuum was generated to outline better the star forming regions.

The continuum level was determined by measuring the counts for several stars common to both the continuum and the line plus continuum images. The selected from the *JHK* color-magnitude diagrams stars were main sequence foreground stars with photometric colors close to those of

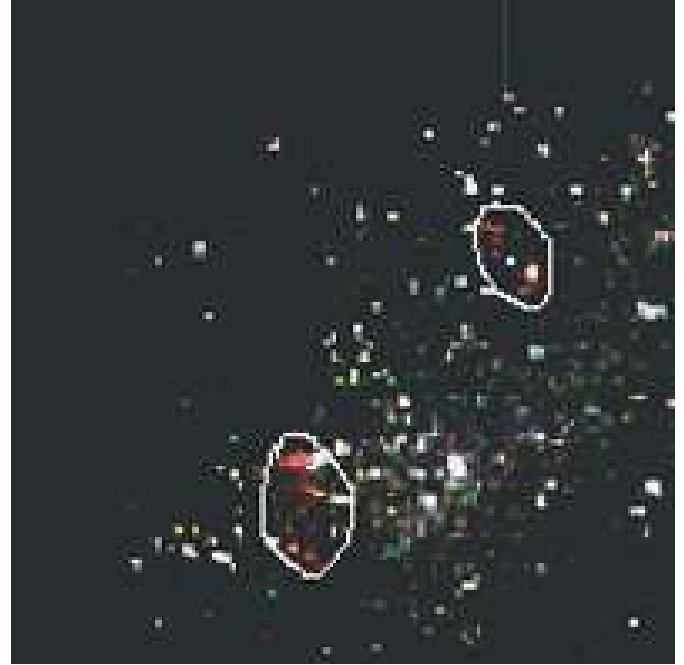


Fig. 14. The red-green-blue composite true color image generated from the H_2 — $2.122\mu\text{m}$ (blue), continuum — $2.26\mu\text{m}$ (green) and $\text{Br}\gamma$ — $2.165\mu\text{m}$ (red) images. North is at the top and east to the left. The field of view as shown is 3.6 arcmin.

spectral class A0. The calculated ratios of counts were then averaged and the continuum image was scaled to the line plus continuum image so that the average ratio is unity. The continuum image was then subtracted from the line plus continuum image. Since the subtraction of continuum is a very important step we checked our results using the method of Golev et al. (1996).

The emission structures are marked on Fig. 15. The lowest and the highest contours correspond to 3σ and 10σ respectively above sky value. Six "knots" and "spots" with diameters twice greater than FWHM can be located above the 3σ sky value. Their measured positions in α_{2000} , δ_{2000} , size in arcsec and fluxes per area per sec are given in Table 1. The $\text{Br}\gamma$ emission sources are rather compact with sizes not larger than 20 arcsec. Br1, Br2 and Br3 have diffuse morphology while Br4, Br5 and Br6 are stellar-like objects.

It is well known that the $\text{Br}\gamma$ recombination line of hydrogen traces sources of Lyman continuum flux i.e. hot young stars. The observed six $\text{Br}\gamma$ emission structures clearly delineate two star forming regions in the galaxy.

9. Summary

The infrared photometry presented here together with the $\text{Br}\gamma$ recombination line images provide useful information on the star-formation episodes of the Local group dwarf irregular galaxy IC 10. The red giants were formed several

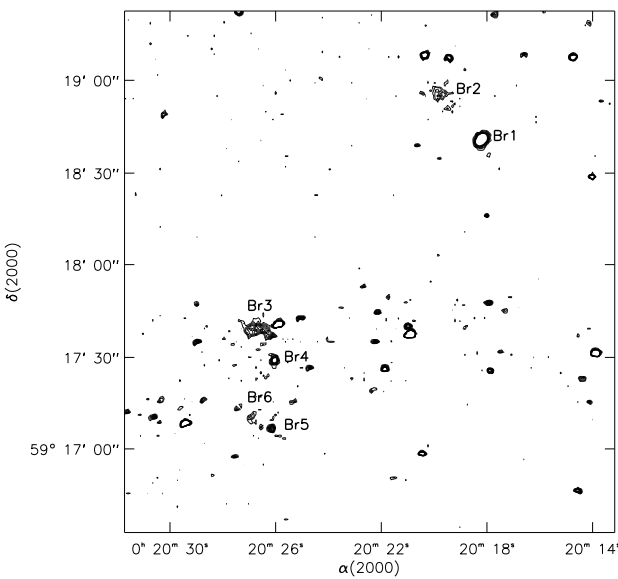


Fig. 15. Contour plot of Br γ - Continuum image. The lowest contour corresponds to 3σ above sky value, the highest contour to 10σ .

Table 1. Bracket gamma emission structures

Name	α_{2000} $00^{\text{h}} +$	δ_{2000} $59^{\circ} +$	Size (arcsec)	Flux (erg cm $^{-2}$ sec $^{-1}$)
Br1	$20^{\text{m}} 18^{\text{s}} 15^{\text{m}}$	$18' 39'' 9$	15.3	$4.44 \cdot 10^{-14}$
Br2	$20^{\text{m}} 19^{\text{s}} 74^{\text{m}}$	$18' 55'' 2$	15.3	$2.41 \cdot 10^{-14}$
Br3	$20^{\text{m}} 26^{\text{s}} 69^{\text{m}}$	$17' 37'' 6$	22.1	$5.63 \cdot 10^{-14}$
Br4	$20^{\text{m}} 26^{\text{s}} 04^{\text{m}}$	$17' 28'' 4$	8.5	$1.24 \cdot 10^{-14}$
Br5	$20^{\text{m}} 26^{\text{s}} 13^{\text{m}}$	$17' 05'' 4$	3.4	$4.25 \cdot 10^{-15}$
Br6	$20^{\text{m}} 26^{\text{s}} 87^{\text{m}}$	$17' 09'' 6$	4.2	$3.25 \cdot 10^{-15}$

Gyr ago with masses up to $7 M_{\odot}$. The derived metallicity ($[\text{Fe}/\text{H}] = -1.60 \pm 0.27$) of the red giants shows that they are relatively metal poor. The red supergiants have masses between 12 and $25 M_{\odot}$ and ages less than 100 Myr. Most of the stars are embedded in gas and dust which results in a very noticeable internal variable reddening. We have determined the mean foreground reddening $E(B - V) = 0.88 \pm 0.11$ of IC 10 and the dereddened distance modulus $(m - M)_0 = 24.0 \pm 0.2$ mag. The Br γ emission structures outline two star forming regions and taking into account the large number of WR stars we confirm the hypothesis of a recent star burst in IC 10.

Acknowledgements. L. G. and J. B. would like to thank Anabel Arieta and Alicia Porras for her help in the process of reducing the IR frames and also E. Chelebiev for his help. The authors gratefully acknowledge the useful comments and suggestions raised by Drs. F. Ferraro, M. R. Cioni, V. Golev, T. Bonev and V.D. Ivanov. This work was performed while J.B. was a visiting astronomer in UNAM, Mexico under contacts CONACYT No.400354-5-2398PE and DGAPA INI04696 and

was supported in part by the Bulgarian National Science Foundation grant under contract No. F-812/1998 with the Bulgarian Ministry of Education and Sciences.

References

Bahcall, J. N., Soneira, R. M. 1980, *ApJS*, 44, 173

Bessell, M., Brett, J. 1988, *PASP*, 100, 1134

Bertelli, G., Bressan, A., Fagotto, F., Chiosi, C., Nasi, E., 1994, *AAS*, 106, 275

Bohlin, R., Colina, L., Finley, D., 1995, *AJ*, 110, 1316

Braun et al., 1998, *PASP*, 110, 810

Casali, M. , Hawarden, T., 1992, *JCMT-UKIRT* Newsletter, No. 3, p. 33

Charbonnel, C., Maynet, G., Maeder, A., Schaller, G., Schaefer, D., 1993, *AAS*, 101, 415

Cohen, R. J., 1979, *MNRAS*, 187, 839

Costa, D., Frogel, G., 1996, *AJ*, 112, 2607

Cruz-Gonález, I., Salas, L., & Ruiz, E., 1996 , Manual de Usuario 96-02, Instituto de Astronomía, UNAM

Elias, J., Frogel, J., Humphreys, R., Persson, S., 1981, *ApJL*, 249, 55

Elias, J., Frogel, J., 1985, *AJ*, 289, 141

Freedman, W., 1988, *AJ*, 96, 1248

Georgiev, L., Borissova, J., Rosado, M., Kurtev, R., et al., 1999, *AAS*, 134, 21

Golev, V., Jankulova, V., Bonev, T., 1996, *MNRAS*, 280, 29

Hubble, E., "The realm of the nebulae", 1936, Yale University Press, New Haven.

Hunter, 1997, *PASP*, 109, 937

Kingsburgh, R., Barlow, M., 1995, *AA*, 295, 171

Koornneef, J., 1983, *AAp*, 128, 84

Kuchinski, L., Frogel, E., Tendrup, D., Persson, S., 1995, *AJ*, 109, 1113

Kuchinski, L., Frogel, J., 1995, *AJ*, 110, 2844

Landolt, A., 1992, *AJ*, 104, 1

Massey, P., Armandroff, T., 1995, *AJ*, 109, 2470

Massey, P., Lang, C., DeGioia-Eastwood, K., Garmány, C., 1995, *ApJ*, 438, 188

Mateo, M., 1998, *ARA&A*, 36, 435

Ruelas-Mayorga, A., 1997, *RevMexAA*, 33, 9

Oke, J., 1990, *AJ*, 99, 1621

Petitpas, G., Wilson, Ch., 1998, *ApJ*, 496, 226

Saha, A., Freedman, W., Hoessel, J., Mossman, A., 1992, *AJ*, 104, 1072

Saha, A., Hoessel, J., Krist, J., Danielson, E., 1996, *AJ*, 111, 197

Sandage, A., 1971, *ApJ*, 166, 13

Shostak, G.S., Skillman, E.D. , 1989, *AA*, 214, 33

Sakai, S., Madore, B., Freedman, W., 1998, *astro-ph/9809025*, in press

Stetson, P., 1993, User's Manual for DAOPHOT II.

Stetson, P. 1991, in *The Formation and Evolution of Star Clusters*, ASP Conf. Ser. Vol. 13, edited by K. A. Janes (ASP, San Francisco), p. 88

Tiede, G., Martini, P., Frogel, J., 1997, *AJ*, 114, 694

Wilson, C., Welch, D., Reid, I., Saha, A., Hoessel, J., 1996, 111, 3

Wilcots, E., Miller, B., 1998, *AJ*, 116, 2363